Accepted Manuscript

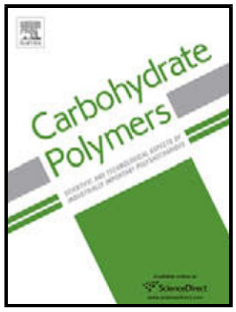

Title: Effect of gum arabic-modified alginate on physicochemical properties, release kinetics, and storage stability of liquid-core hydrogel beads

Authors: Fu-Hsuan Tsai, Yutaka Kitamura, Mito Kokawa

PII: S0144-8617(17)30797-X
DOI: http://dx.doi.org/doi:10.1016/j.carbpol.2017.07.031
Reference: CARP 12548

To appear in:

Received date: 20-3-2017
Revised date: 7-7-2017
Accepted date: 11-7-2017

Please cite this article as: Tsai, Fu-Hsuan., Kitamura, Yutaka., & Kokawa, Mito., Effect of gum arabic-modified alginate on physicochemical properties, release kinetics, and storage stability of liquid-core hydrogel beads.*Carbohydrate Polymers* http://dx.doi.org/10.1016/j.carbpol.2017.07.031

This is a PDF file of an unedited manuscript that has been accepted for publication. As a service to our customers we are providing this early version of the manuscript. The manuscript will undergo copyediting, typesetting, and review of the resulting proof before it is published in its final form. Please note that during the production process errors may be discovered which could affect the content, and all legal disclaimers that apply to the journal pertain.

ACCEPTED MANUSCRIPT

Effect of gum arabic-modified alginate on physicochemical properties, release kinetics, and storage stability of liquid-core hydrogel beads

Fu-Hsuan Tsai[a], Yutaka Kitamura[b*], Mito Kokawa[b]

[a] Graduate School of Life and Environmental Sciences, University of Tsukuba, 1-1-1 Tennodai, Tsukuba, Ibaraki 305-8577, Japan.

[b] Faculty of Life and Environmental Sciences, University of Tsukuba, 1-1-1 Tennodai, Tsukuba, Ibaraki 305-8577, Japan.

*Corresponding Author. Tel.: +81 298 53 4655, Fax.: +81 298 53 4655

Email: kitamura.yutaka.fm@u.tsukuba.ac.jp

Highlights

- Alginate/ gum arabic beads (AGB) were prepared by reverse spherification.
- Release behavior and release kinetics in an *in vitro* system were investigated.
- Storage stability and release behavior of total phenolic compounds were improved.
- AGB may serve as a potential carriers of radish by-product juice.

Abstract

Different weight ratios of alginate/gum arabic (GA) solutions were prepared to serve as the wall material of liquid-core hydrogel beads (LHB) that were formulated to protect the total phenolic compounds (TP) of radish by-product juice from degradation during storage and release in simulated gastrointestinal fluid. The diameter of LHB ranged from 4.63 to 5.66 mm with a sphericity lower than 0.05. LHB formulated with 25 % GA (AGB0.25) exhibited the highest

ACCEPTED MANUSCRIPT

hardness (26.63 N), and those formulated with 50 % GA (AGB0.50) exhibited the highest loading efficiency (86.67 %). AGB0.25 was effective in preventing TP from degrading during storage with a decay rate (k) of 6.10×10^{-3} day^{-1} and a half-life ($t_{1/2}$) of 113.63 days, it showed the slowest release of TP in simulated gastric fluid (k=2.25×10^{-6}), and the release mechanism followed Fickian diffusion. The results suggest that GA is effective in improving the physicochemical properties of alginate.

Abbreviations

AGB: alginate/gun arabic bead; ANOVA: analysis of variance; AOAC: Association of Official Agricultural Chemists; CL: calcium lactate; G residues: α-L-guluronic acid unit of SA; GA: gum arabic; GRAS: generally regarded as safe; USFDA: United States Food and Drug Administration; LCM: liquid-core material; LHB: liquid-core hydrogel beads; M residues: β-D-mannuronic acid unit of SA; MWM: micro wet milling system; RBJ: radish by-product juice; RSM: response surface methodology; RVS: reverse spherification; SA: sodium alginate; SIF: simulated intestinal fluid; SGF: simulated gastric fluid; TP: total phenolic compounds; USP: United States pharmacopeia.

Keywords:-radish by-product, micro wet milling, gum arabic, encapsulation, reverse spherification, *in vitro* release

1. Introduction

Much attention has been focused on hydrogel bead formed by food-grade biopolymers as a delivery system to protect and encapsulate some food ingredients, drugs, and bioactive compounds and/or control their release behavior (Gouin, 2004; Matalanis, Jones, & McClements, 2011).

ACCEPTED MANUSCRIPT

Alginate is a natural linear biopolymer consisting of 1,4-linked β-D-mannuronic (M residues) and α-L-guluronic acids (G residues) and divided into homopolymeric blocks (G- and M-blocks) and heteropolymeric blocks (MG-blocks) (Pawar & Edgar, 2012). Normally, it is extracted from brown algae; however, in order to obtain a more flexible structure and better physical properties, alginate has been recently shown to be able to be produced by bacterial biosynthesis (Lee & Mooney, 2012). Alginate is widely used in the food, medical, and pharmaceutical industries due to its non-toxicity, relatively low cost, simple preparation, high compatibility, and biodegradability (Zeeb, Saberi, Weiss, & McClements, 2015). Alginate undergoes ionotropic gelation and forms egg-box dimers due to the interaction between G-blocks and some cations, such as Cu^{2+}, Zn^{2+}, Ca^{2+}, Ba^{2+}, and Al^{3+}. Egg-box dimers further aggregate and compose egg-box multimers (Fang et al., 2007; Nayak, Das, & Maji, 2012). Ionotropically gelled alginate is a pH-sensitive polymer that shrinks in acidic conditions and swells in a high-pH environment (Wang, Zhang, & Wang, 2009). This characteristic makes alginate widely used for the delivery of proteins, drugs, and probiotics, protecting these compounds from destruction by stomach fluid (Cai et al., 2014; Mohy Eldin, Kamoun, Sofan, & Elbayomi, 2014).

Reverse spherification (RVS), one of the encapsulation methods, is used for preparing liquid-core hydrogel beads (LHB). The method is performed by dripping droplets that contain ions and bioactive compounds, into an ionotropic polymer solution. The most common materials are Ca^{2+} and alginate. RVS is divided into two steps, the first and secondary gelations (Fu Hsuan Tsai, Chuang, Kitamura, Kokawa, & Islam, 2017). The first gelation is a step of LHB formation, in which Ca^{2+} release from droplets forms a water-insoluble coating (calcium alginate). The thickness of the coating layer increases with time until the osmotic pressures are balanced. Next, these semifinished beads are transferred into a Ca^{2+} solution for secondary gelation, where Ca^{2+} permeates into the network of coating layer. Ca^{2+} fills into the G blocks that were not combined with Ca^{2+} in first gelation, and the stability and hardness of coating layer increases. Thus,

ACCEPTED MANUSCRIPT

secondary gelation is defined as a hardening step. In our previous study, the conditions of LHB formulation by response surface methodology (RSM) was optimized to investigate the effects of first and secondary gelation on different physical properties (Fu Hsuan Tsai, Kitamura, & Kokawa, 2017). Our studies demonstrated that LHB prevents the DPPH-scavenging ability of functional compounds from decreasing during storage (F. H. Tsai, Chiang, Kitamura, Kokawa, & Khalid, 2016) and examined the release profiles of functional compounds in simulated gastrointestinal fluid (*in vitro*) and during thermal treatments (Fu Hsuan Tsai, Chuang, et al., 2017). These results indicated that alginate could be used as a potential delivery method; however, properties such as loading efficiency, hardness, and release characteristics in gastric fluid could be improved for more efficient delivery. Amine et al. (2014) indicated that ionotropically gelled alginate has a high permeability and entrapped compounds are released from alginate hydrogel beads rapidly due to their hydrophilic and porous structure.

Some studies have reported that improving physicochemical properties by adding other polymers as fillers, such as tapioca starch, chitosan and gum arabic (Chopra et al., 2015; Lozano-Vazquez et al., 2015; Mukhopadhyay, Chakraborty, Bhattacharya, Mishra, & Kundu, 2015). Gum arabic (GA), also known as gum acacia, is a highly branched natural polymer formulated from the tree sap of Acacia Senegal trees. The main chain of GA consists of β-D-galactopyranosyl units and side chains are formed of L-arabinose, L-rhamnose, D-galactose, and D-glucuronic acid (Chopra et al., 2015; Nayak et al., 2012). It is widely used as stabilizer, thickening agent, hydrocolloid emulsifier, and carrier in food, pharmaceutical, and cosmetic industries (Nami, Haghshenas, & Yari Khosroushahi, 2016).

Alginate and GA are both biodegradable and biocompatible polymers as well as generally regarded as safe (GRAS) by the United States Food and Drug Administration (USFDA). Fang et al. (2011) indicated that in the case of dry alginate beads, the addition of gum arabic reduced the side-by-side aggregation of the egg-box structure of the alginate. Side-by-side aggregation

ACCEPTED MANUSCRIPT

occurs when calcium alginate is dried. The egg-box junctions are drawn together due to the collapse of the alginate network, which results in further combining of the egg-box junctions by the presence of calcium ions. Side-by-side aggregation leads to a loss of the swelling capacity of calcium alginate. The combination of alginate and GA has attracted attention for the protection of probiotic bacteria and drugs during drying, storage, and in the gastric tract (Chopra et al., 2015; Nami et al., 2016; Nayak et al., 2012). However, to our knowledge, little or no information is currently available on the LHB prepared by alginate/GA matrix.

Preparing LHB by RSV has received increased attention in recent years. Materials which have high functionality and are suitable for RVS processing have been searched for. This work is the first paper to prepare LHB from alginate combined with GA by RVS. The objective of this work was to investigate a delivery of vegetable extract in an attempt to protect its functional compounds from being destroyed in gastrointestinal tracts and during storage. The first physical properties that were evaluated were the diameter, sphericity, and loading efficiency of the alginate/GA bead (AGB). The change of hardness, total phenolic compounds (TP) release behavior, and release kinetics in an *in vitro* system were also investigated. Finally, the stability of stored TP, including their antioxidant ability and degradation kinetics, were examined.

2. Materials and Methods

2.1. Materials

Radish (*Raphanus sativus* L.) is an important root vegetable crop worldwide because of its high nutritional and medicinal value. Furthermore, radish leaves have an abundance of minerals and the content of phenolic compounds and flavonoids in leaves are approximately 2.0-fold and 3.9-fold that of their content in roots, which are the parts which are normally consumed (Goyeneche et al., 2015). Radish leaves are seldomly consumed because of their bitter taste and strong flavor, despite containing an abundance of nutrients.

ACCEPTED MANUSCRIPT

Radish leaves were obtained from a local farmer. The cleaned leaves were cut and stored at -20°C. Sodium alginate (SA), GA, chitosan 100, acetic acid, calcium lactate (CL), ethanol, sodium chloride (NaCl), hydrochloric acid (HCl), and sodium carbonate (Na_2CO_3) were purchased from Wako Pure Chemical Industries, Ltd. (Japan). The viscosity of a 1 % solution of SA was 80-120 m Pa・s at 20°C, the molecular weight was 1325 kDa, the percentage of guluronate content was 34.4 %, and guluronate–guluronate diad frequency was 18.9 % (Nakata, Kyoui, Takahashi, Kimura, & Kuda, 2016). The viscosity of 1 % GA was 3.1 mPa・s at 20°C. The molecular weight of chitosan 100 was approximately 1.3×10^5 Da and the degree of deacetylation was 78 % (Bhattarai, Bahadur K.C., Aryal, Khil, & Kim, 2007). Pepsin (1:10,000, from porcine stomach mucosa) and pancreatin U.S.P. were purchased from MP Biomedicals, Inc. (USA). Folin-Ciocalteu reagent was purchased from Merck Millipore Corporation (USA). α,α-diphenyl-β-picrylhydrazyl (DPPH) was purchased from Sigma-Aldrich (USA). All chemicals in the investigation were of analytical grade.

2.2. Preparation of alginate/GA bead (AGB) and storage test

AGB is a hydrogel bead that is composed of an alginate/GA outer layer and a liquid -core consisting of radish by-product juice (RBJ), chitosan and acetic acid. RBJ was prepared by mixing radish leaves and distilled water at a ratio of 1:2 in a blender at approximately 15,000 rpm for 1 min and then feeding that mixture into a micro wet milling system (MWM) by a tubing pump at 10 mL/min. The MWM grinds samples by using two stacked milling stones. The lower milling stone was rotated by an electric motor at 30 rpm and the upper milling stone was fixed on the system. RBJ was ground by the shear and frictional stress between two milling stones, and the particle size reached micrometer scale (Koyama & Kitamura, 2014). The liquid-core material (LCM) was formulated by mixing 2 % chitosan and 1 % acetic acid in RBJ to reach a final concentration of 0.12 M CL solution. Chitosan was used as a thickener to modulate

ACCEPTED MANUSCRIPT

the viscosity and density of the LCM to prevent it from being deformed by shear stress during first gelation. The wall materials of AGB were prepared from 100 mL of solutions containing 1 g of SA and different amounts of GA (0.00, 0.33, 1.00, and 3.00 g), to achieve alginate/GA weight ratios of 0/1, 0.25/0.75, 0.5/ 0.5, and 0.75/0.25, respectively. These different variations of AGB were coded as AGB0, AGB0.25, AGB0.5, and AGB0.75, respectively (Table 1).

The preparation of AGB was separated into the two steps of gelation (Fig. 1). In the first gelation, LCM was extruded into different wall materials through a 20G flat-tipped hypodermic needle with gentle stirring for 25 min. The semifinished beads were collected and washed with distilled water and 95 % ethanol, and then secondary gelation was carried out. In the secondary gelation, semifinished beads were suspended in 0.05 M CL solution for 6 min, and then AGB was prepared by collecting and rinsing these beads with distilled water and 95 % ethanol again. The different varation of AGB were stored for 0 to 28 days at 4°C for evaluating the TP loss and decrease in antioxidant ability during storage.

2.3. Diameter and sphericity

Images of the AGB was recorded with a digital camera. The diameter of AGB was measured by ImageJ software (version 1.50i, National Institutes of Health, USA) and the sphericity was calculated with the following equation:

$$\text{Sphericity} = (d_{max} - d_{min})/(d_{max} + d_{min})$$

where d_{max} and d_{min} are the largest and the smallest diameters of the same bead, respectively (López Córdoba, Deladino, & Martino, 2013).

2.4. Total phenolic content and loading efficiency

ACCEPTED MANUSCRIPT

AGB (0.5 g) or LCM (1 mL) was added to 10 mL of 1 % acetic acid, mixed by a homogenizer (NS-52K, Microtec, Japan) at 10,000 rpm for 30 s, and centrifuged at 4000 rpm for 5 min. The amount of TP in the supernatant was determined with Folin-Ciocalteu method (Goyeneche et al., 2015). The supernatant (0.5 mL) was mixed with 0.5 of Folin-Ciocalteu reagent and 2 mL of 20 % of Na_2CO_3 solution. The mixture was left at room temperature for 15 min and entrifuged at 4000 rpm for 5 min. The absorbance of a sample was measured at 725 nm by a spectrophotometer (U-1900, Hitachi, Japan). Loading effieiency was calculated as follows:

$$\text{Loading efficiency } (\%) = \text{TP amount in AGB}/\text{TP amount in LCM} \times 100$$

TP loss during storage was evaluated by a first-order kinetic model,

$$lnM_t = lnM_0 - kt$$

and the reduction rate (k) and half-life ($t_{1/2}$) were calculated using,

$$t_{1/2} = ln2/k$$

where M_t and M_0 are the amounts of TP at days t and 0, respectively.

2.5. Antioxidant ability

The antioxidant activity of AGB during storage was determined by DPPH assay. DPPH, a stable free radical, is widely used to evaluate the antioxidant abilities of phenols by capturing H atoms of phenols (Achat, Rakotomanomana, Madani, & Dangles, 2016). The DPPH-scavenging activity was determined by the method of Lai, Chou, & Chao (2001). The decrease of DPPH-scavenging activity during storage, reduction rate (k) and half-lives ($t_{1/2}$) were evaluated by formula in section 2.4. AGB (0.5 g) or LCM (1 mL) was blended and centrifuged as described in the method of section 2.4. An aliquot of 1 mL of 0.2 mM DPPH in methanol was mixed with 1 mL of the supernatant. The mixture was mixed by vortexing and left in the dark for 30 min at room temperature. The absorbance of a sample (A_s), control (sample was replaced by distilled water, A_c), and blank (A_b) were measured by a spectrophotometer at 517 nm. DPPH-scavenging

ACCEPTED MANUSCRIPT

activity was calculated with the following equation:

$$\text{DPPH} - \text{scavenging activity}\ (\%) = [1 - (A_s - A_b)/A_c] \times 100$$

2.6. *In vitro* release profile and release kinetic

In vitro release experiments were performed by the method of Tsai, Chuang, Kitamura, Kokawa, & Islam (2017), using United States Pharmacopeia (USP) apparatus 2 (PJP-32N, Miyamoto Riken, Japan). Simulated gastric fluid (SGF) was prepared by mixing 2 g of NaCl, 3.2 g of pepsin, and 7 mL of HCl in 500 mL of distilled water, and adding distilled water to 1 L, simulated intestinal fluid (SIF) was prepared by mixing 6.8 g of NaOH, 77 mL 0.2 N of KH_2PO_4, and 10 g of pancreatin, and adding distilled water to reach 1 L. AGB (0.5 g) was left in 300 mL of SGF for 120 min and then transferred to SIF for 240 min at 37 ˚C, with a paddle rotation speed of 50 rpm. Aliquots of 1 mL of the medium were withdrawn at specified times and replaced with fresh release medium. The TP amount in the medium was measured by the method of section 2.4.

The release mechanisms of TP were evaluated with the Korsmeyer-Peppas model (Korsmeyer, Gurny, Doelker, Buri, & Peppas, 1983):

$$M_t/M_\infty = kt^n$$

where M_t is the amount of TP at time t, M_∞ is the total amount of TP in AGB, *k* is the release kinetic constants, and *n* is the release exponent, indicative of the drug release mechanism.

2.7. Hardness

A compression test was carried out with a texture analyzer (EZ-SX 100N C05 KIT, Shimadzu Ltd. Japan) at room temperature. A 25 mm cylinder probe was used to compress the AGB with a test speed of 20.0 mm/min to 4 mm from the start position, when the probe stopped and returned to start position. The maximum force (N) of compression was represented as the

ACCEPTED MANUSCRIPT

hardness of AGB (Belščak-Cvitanović et al., 2015). Relative hardness was calculated with the following equation, using AGB0 as a standard:

$$\text{Relative hardness (\%)} = \text{Hardness of each variation} / \text{Hardness of AGB0} \times 100$$

2.8. Glass transition temperature (T_g)

The T_g values of the beads were measured according to the method of Lupo, Maestro, Gutiérrez, & González (2015) with some modifications. Alginate/GA beads were dried by a freeze dryer (FD-1, Tokyo Rikakikai, Japan) for 12 h. Approximately 3 mg of dried alginate/GA outer layer was removed from AGB and sealed in an aluminum sample pan. The T_g of alginate/GA outer layer was determined by a differential scanning calorimetry (DSC-60, Shimadzu Corporation, Japan). The sample was heated from 20 ˚C to 300 ˚C at a rate of 10 ˚C/ min with a flow rate of 30 mL/min of nitrogen and taking an empty aluminum pan as a reference. Moisture content, which was determined by AOAC method (AOAC, 2000), of the fresh out layer of AGB0, AGB0.25, AGB0.5, and AGB0.75 were 96.93 %, 96.84 %, 96.12 %, and 93.87%, respectively.

2.9. SEM microscopy

Dry AGB were prepared with a freeze dryer as described in the section 2.8. and then fixed on an stub with double-sided adhesive tape. The beads were coated with a platinum–palladium with a sputter coater (E-1045, Hitachi, Japan) under vacuum for 1 min. The microstructure of the AGB surface was observed by a scanning electron microscope (JSM-6330F, JEOL, Japan) with accelerating potential of 5kV.

2.10. Statistical analysis

All experiments were run at least in triplicate. The results were presented as the mean± standard deviation and analyzed using Statistical Analysis System software (Version 8.01, SAS Institute

ACCEPTED MANUSCRIPT

Inc., USA). One-way analysis of variance (ANOVA), followed by Duncan's multiple comparison test, was performed. Responses with p values <0.05 were considered significant.

3. Results and Discussion

3.1. Characterization of AGB

In this section, the diameter, sphericity, and loading efficiency were used to evaluate the physicochemical properties of AGB (Table 2). The diameter of AGB ranged from 4.63 to 5.66 mm. There was no significant difference between AGB0 and AGB0.25 as well as between AGB0 and AGB0.5 ($p<0.05$); however, AGB0.75 showed a relatively larger diameter. Our former study (F. H. Tsai et al., 2016) demonstrated that semifinished beads tended to shrink during secondary gelation because alginate in the outer layer of AGB were pulled together by calcium ions. We inferred that AGB0.75 showed a relatively higher diameter, which is similar to that of semifinished beads, because GA was a barrier to the combining of alginate.

Sphericity is an efficiency factor that evaluates the roundness of hydrogel beads. A higher value indicates a greater degree of deformation, and a value of zero indicates a perfect sphere. A hydrogel bead is considered a sphere if the sphericity is lower than 0.05 because the shape distortion cannot be obviously distinguished by human vision (Chan, Lee, Ravindra, & Poncelet, 2009; Chew & Nyam, 2016). AGB0 had a higher sphericity than the other variations. During the first gelation, which has been demonstrated to be the shape-determining step, the droplet of LCM is extruded from a syringe with a needle into the wall material solution. The LCM is not a perfect sphere and is fragile to deformation as it passes through the surface of wall material solution, but returns to a spherical shape during in an appropriate first gelation time. We inferred that the reason that AGB0 has a higher sphericity is because the conjugation of alginate without the interference of GA was so fast that LCM could not return to a perfect sphere before the shape was set. However, the sphericity of all the variations were lower than 0.05, and they could

ACCEPTED MANUSCRIPT

thus, be considered as spheres.

Loading efficiency was expressed as the ratio between the TP content in AGB and the TP content in LCM, the total amount used to prepare AGB. Low loading efficiency could lead to a high cost of preparation and a less valuable product (Zucker, Marcus, Barenholz, & Goldblum, 2009). According to Table 2, AGB0.5 showed the highest loading efficiency (86.67 %), which was higher than that of AGB0 (83.80 %). The result showed that the addition of GA could improve the loading efficiency of alginate beads. The study of Chopra et al. (2015) also indicated that the encapsulation efficiency of alginate beads is increased by adding a proper concentration of GA because of the interaction between alginate and GA. Furthermore, the wall material of the alginate and GA mixture has a higher viscosity, preventing the TP release during preparation (Nayak et al., 2012). However, increasing the GA ratio greater than AGB0.5 decreases the loading efficiency. It was attributed to GA being unable to undergo gelation by itself; therefore, TP leaks out from AGB that contain a high amount of GA in the wall material (Fang et al., 2011).

Means of 3 replicates ± standard deviation.

[a-c] Means within the same column of each treatment with different superscript letters are significantly different at $p < 0.05$.

3.2. Degradation of total phenolic compound

The TP amount was expressed as the amount of TP found in AGB on a specific day of storage relative to the total amount of TP used to prepare AGB. Fig. 2 illustrates the decrease in TP during a storage test. The TP amount in AGB was lower than that in LCM due to TP loss during preparation. After 28 days of storage, there was no significant difference between TP amounts of AGB0.25 (72.46 %) and LCM (72.29 %).

ACCEPTED MANUSCRIPT

TP degradation was evaluated by the first-order kinetic model, and the kinetic parameters obtained are shown in Table 3. The results were well fit by the first-order kinetic model, indicated by the high (0.957 to 0.988) values of correlation (R^2). LCM had a high TP amount after 28 days of storage but the relatively higher *k* value (1.11×10^{-2} day^{-1}) showed that TP was easily destroyed when it was not protected by alginate or alginate/GA outlayer. LH0 showed a lower *k* value than LCM. LH0.25 showed a low *k* value, but the *k* value increased from 6.10×10^{-3} to 1.03×10^{-2} day^{-1} with as the GA ratio increased. The half-life ($t_{1/2}$) value indicates the days that were required for the TP amount to be reduced by half. The half-life of TP in LH0.25 was more than 100 days but the half-life of TP without alginate or alginate/GA outlayer protection (LCM) was only approximately 62 days. The result demonstrated that AGB were good at preventing TP degradation during storage.

3.3. Antioxidant activity

At the beginning of storage, the DPPH-scavenging ability of AGB varied between 75.37 % and 89.56 % and was lower than LCM (96.17 %) (Fig. 3). After 28 days of storage, the DPPH-scavenging ability of AGB0.25 and AGB0.5 were higher than 70 %, on the other hand, AGB0.75 showed the lowest DPPH-scavenging ability.

DPPH-scavenging ability reduction was found to be fit by first-order kinetics with high correlation (R^2) (0.929 to 0.961) (Table 3). Hydrogel beads without GA (AGB0) showed that their DPPH-scavenging ability decay rate was 1.01×10^{-1} day^{-1} and their half- life was 68.63 days. AGB0.25 resulted in a slower decay rate of DPPH-scavenging ability ($k= 8.00\times10^{-3}$ day^{-1}) and a longer shelf- life (half- life of 86.64 days); however, as the ratio of GA increased, the

ACCEPTED MANUSCRIPT

decay rate of DPPH-scavenging ability increased and the half-life decreased. Tonon, Brabet, & Hubinger (2010) also indicated that anthocyanins in non-encapsulated black berry juice showed a higher degradation rate due to a greater contact with oxygen. Oxidation is one of the causes of TP degradation; however, AGB could eliminate the direct contact between core materials and environmental factors. The trend of the DPPH-scavenging ability decrease was similar to the trend of the amount of TP (**Error! Reference source not found.**). Phenolic compounds play an important role in antioxidant ability; therefore, more TP resulted in a higher DPPH-scavenging ability. We investigated the correlation between DPPH-scavenging activity and TP amount, and the result is shown in Fig. 4. It was found that DPPH-scavenging activity positively correlated with the amount of TP ($R^2 = 0.92$).

3.4. *In vitro* release profile and kinetics

The release behavior of AGB was investigated by an *in vitro* drug release experiment. Alginate/GA beads were soaked in SGF (pH 1.2) for 2 h and then transferred to SIF (pH 6.8) for 4 h. The appropriate technologies and materials of bead preparation should be chosen to effect ideal release behavior. Because of its pH-sensitivity, biocompatibility, and ease of manipulation, alginate has been widely used for carrying environmentally sensitive bioactives and oral delivery systems (Burey, Bhandari, Howes, & Gidley, 2008; Gong et al., 2011; Zeeb et al., 2015). Some articles also report that the presence of pores in the alginate network is the major factor for release. The use of filler for delaying active compound release was deescribed (López Córdoba et al., 2013). To prevent core material from being destroying and releasing into stomach fluid, we tried to prepare a delivery system that can coat bioactives and protect them in SGF, for transport to the SIF. Bioactives were expected to be released and absorbed in the intestinal tract. Thus, a low amount and slow release of TP in SGF was favored for this study. IN constrast, a high amount and high-speed release of TP in SIF was expected. GA was used as

ACCEPTED MANUSCRIPT

a filler in this work because of its ampholytic characteristics (Fang et al., 2011).

The effect of the alginate to GA ratio on the TP release profile is shown in Fig. 5. Alginate tends to shrink and has poor water solubility in acidic pH (Sinha, Ubaidulla, Hasnain, Nayak, & Rama, 2015), slowing the release of the compound from AGB. With the increase in GA, the amount of TP released from AGB in SGF decreased for 2 h and then increased. AGB0.75 showed the highest amount of TP release (53.15 %), which was about two times higher than that of AGB0.25 (27.42 %) in the same time interval. The result indicates that a proper alginate to GA ratio can prevent TP release because GA play a role as a barrier in the pores in alginate (Nayak et al., 2012).

According to Fig. 5, the amount of TP released by AGB0.75 did not show any significant change after 180 min, AGB0 and AGB0.25 did not show any significant change after 300 min, and AGB0.5 did not show any significant change after 210 min ($p<0.05$). The result indicates that the amount of TP released for all variations reached their maxima in 6 h. AGB0 released approximately 89 % of its TP in 6 h. On the other hand, the amount of TP released by all variations of AGB was higher than 90 %. If TP are not released from hydrogel beads within 6 h in an *in vitro* release system, they could form waster by exiting the body through the waste system. The results demonstrated that the addition of GA could modify the release behavior of alginate.

The release profile was analyzed by fitting the results of the curve to the Korsmeyer-Peppas model, and the results were given in

ACCEPTED MANUSCRIPT

Table **4**. Korsmeyer-Peppas is a simple but useful formulation to evaluate release mechanisms (Costa & Sousa Lobo, 2001). For a sphere, the release mechanism follows Fickian release when the release exponent (*n*) is approximately 0.43, when the *n* values are between 0.43 and 0.85, the release is defined as anomalous transport, and the release mechanism is defined as case-II transport when *n* is approximately 0.85. Fickian release indicates a diffusion-controlled release, in which compounds release from delivery by diffusion, anomalous transport represents a non-Fickian release, and case-II transport indicates a swelling-controlled release, in which water plays a role as a plasticizer (Siepmann & Peppas, 2001). The *n* values of all the samples ranged from 0.082 to 0.278, indicating that the release profile follows Fickian release. The release rate of TP in SGF showed an increase and then a decrease with an increasing amount of GA, while AGB0.25 showed the lowest release rate.

GA is an ampholytic polymer. This characteristic makes GA attract alginate molecules, which are negatively charged, with electrostatic forces. Calcium ions do not only play a role as a crosslinker of alginate; they also react with the carboxylate groups of GA (Fang et al., 2011; Nayak et al., 2012).

ACCEPTED MANUSCRIPT

Table **4** also shows that the relatively higher *k* values in SIF were in the range from 2.71×10^{-3} to 6.09×10^{-3} min^{-1}. The result demonstrates that TP were released from AGB were quicker in SIF than in SGF. The faster release in SIF might be due to the pK_a of carboxyl groups (-COOH), which is 4.75, being lower than the pH of SIF (pH 6.8). Carboxyl groups deprotonate to carboxylate anions ($-COO^-$) and hydrogen ions (H^+). The electrostatic repulsive forces between carboxylate anions leads to alginate polymer swelling (Gong et al., 2011). AGB0.75 in SIF was fit worse by Korsmeyer-Peppas models and had the lowest R^2 (0.796) among all the variations. The release amount of TP released by AGB0.75 was over 95 % at 180 min (Fig. 5), and there were no significant difference between TP release amounts from 180 min to 300 min. We inferred that AGB0.75 releases TP in SIF quickly, resulting in a poorer fit to the Korsmeyer-Peppas model.

3.5. Hardness

The effect of the alginate/GA ratio on hardness in an *in vitro* system was evaluated by a compression model in this study. The results are shown in Table 2. A wide range of hardness could be observed by changing the ratios of alginate and GA in the formulation. The hardness of AGB before being soaked in SGF ranged from 6.53 N to 26.68 N, and AGB0.25 showed the highest hardness among all of the variation. Jost, Kobsik, Schmid, & Noller, (2014) indicated that even if alginate is good at holding water and controlling drug release, in addition to being widely used as an air barrier, the brittleness of alginate film is one of the obstacles that needs to be overcome. The results demonstrate that GA has an ability to improve the hardness of alginate beads. However, an increase of GA break the balance of interactions between GA, alginate, and calcium, causing the hardness of AGB to decrease (Chopra et al., 2015). We used the sample of AGB0 before soaking in an *in vitro* system as a standard, and the relative hardness of AGB were calculated (Fig. 6). The hardness of AGB0.75 after 90 min was too low to be

ACCEPTED MANUSCRIPT

detected, and the hardness of other variations ranged from 8.37 to 15.87 % after 120 min. AGB0 remained a relatively higher hardness after being suspended in SGF for 120 min. Furthermore, hardness of all of the variations was too low to be detected after 150 min.

3.6. Characterization of the outer layer of AGB

AGB consists of an alginate or alginate/GA outer layer and a liquid core. The T_g and morphology of the outer layer of AGB were analyzed in this section. The T_g is the temperature at which polymer transitions from the glassy state to the rubbery state occur, and the midpoint temperature of DSC thermogram is considered as the T_g (Mohy Eldin et al., 2014; Pei, Ying, & Chu, 2017). The T_g of alginate/GA outer layers were analyzed and characterized in dry form. A broad endothermic peak was observed between 60 to 120 ˚C. The T_g of alginate/GA outer layers ranged from 68.08 to 82.24 ˚C, and it was found to first increase with the increase of GA ratio and then decrease. The highest T_g was obtained with AGB0.25. Some studies demonstrated that the T_g indicates the interactions between components, a higher T_g indicates a larger interaction between polymer materials (Liu et al., 2012; Lupo et al., 2015). Therefore, we inferred that AGB0.25 has an appropriate balance between alginate and GA, and that the lower T_g of AGB0.75 suggested that the balance was broken by the excess GA.

Abdorreza, Cheng, & Karim (2011) indicated that T_g decreases with the addition of a plasticizer, water plays a plasticizing role; therefore, the T_g decreases with an increase of water content. The T_g of a binary water-solid mixture can be predicted by the Fox equation:

$$1/T_{g,mix} = \omega_1/T_{g1} + \omega_2/T_{g2}$$

where $T_{g,mix}$, T_{g1} and T_{g2} (-148 ˚C) are the glass transition temperature of the mixture, solids, and water, respectively, ω_1 and ω_2 are the mass fraction of solid and water, respectively (Fox, 1956; Wortmann, Rigby, & Phillips, 1984). The T_g of alginate or alginate/GA outer layers ranged from approximately -183 to -163 ˚C.

ACCEPTED MANUSCRIPT

The microstructure of AGB was visualized by SEM (Fig. 7). These SEM photographs reveal some wrinkles on the surface of all variations of AGB, which may be due to the partial collapse of the polymer during freeze drying (Nayak, Pal, & Santra, 2016).

AGB0 had a relatively smoother surface than other treatments (Fig. 7a). With the increase of GA ratio, the surface of AGB became rougher at first, and then became smooth again. The surface of AGB0.25 was roughest, and a ridge structure was observed (Fig. 7b). The ridge structure was also observed on LHB which were prepared by RVS with a high concentration of calcium chloride solution (Fu Hsuan Tsai, Chuang, et al., 2017). Interestingly, this study indicated that LHB in which the ridge structure was observed had a good controlled-release ability. This result is similar to that of this study: AGB0.25, in which a clear ridge structure can be observed, also shows a slow TP release (Fig. 5). Perhaps the ridge structure could be regarded as a feature of LHB indicating good controlled-release ability, although further studies are required for confirmation. AGB0.75 exhibited a very porous surface with some tortuous flake structure (Fig. 7d). The phenomenon resulted in the low loading efficiency and hardness, and a poor ability for slowing down the release of TP of AGB0.75. Some studies have indicated that alginate-based beads are characterized with a porous and collapsed structure (Belščak-Cvitanović et al., 2015). However, this phenomenon was not observed in the most of the AGB except AGB0.75, which indicates that the influence of materials on the morphology of hydrogel beads depends on the preparation method used.

4. Conclusions

This study revealed that GA is a good material to improve the physicochemical properties of alginate hydrogel beads. All of the variations showed a small sphericity (lower than 0.05) and demonstrated that the deformation of AGB is not clearly visible by human eyes. Storage tests confirmed that the addition of GA can prevent TP from degradation, and the results were well

ACCEPTED MANUSCRIPT

fit by a first-order kinetic model, with R^2 ranging from 0.957 to 0.988. GA can also maintain antioxidant activity during storage. *In vitro* release experiments indicated that AGB0.25 has a better performance in preventing TP release in SGF. AGB0.75 showed the highest amount of TP release (53.15 %) in SGF, which was about two times higher than AGB0.25 (27.42 %) in the same time interval. AGB0.25 also shows fine results for the hardness and prolonging half-life of TP degradation during storage, the half-life of TP decay in AGB0.25 is over than 100 days and the hardness was 23.42 N. Thus, these results suggest that AGB can be used as potential carriers of radish by-product juice.

ACCEPTED MANUSCRIPT

Reference

Abdorreza, M. N., Cheng, L. H., & Karim, a. a. (2011). Effects of plasticizers on thermal properties and heat sealability of sago starch films. *Food Hydrocolloids*, *25*(1), 56–60.

Achat, S., Rakotomanomana, N., Madani, K., & Dangles, O. (2016). Antioxidant activity of olive phenols and other dietary phenols in model gastric conditions: Scavenging of the free radical DPPH and inhibition of the haem-induced peroxidation of linoleic acid. *Food Chemistry*, *213*, 135–142.

Amine, K. M., Champagne, C. P., Salmieri, S., Britten, M., St-Gelais, D., Fustier, P., & Lacroix, M. (2014). Effect of palmitoylated alginate microencapsulation on viability of Bifidobacterium longum during freeze-drying. *LWT - Food Science and Technology*, *56*(1), 111–117.

AOAC. (2000). *Official methods of analysis. (17th ed.). Gaithersburg, MD: Association of Official Analytical Chemists*.

Belščak-Cvitanović, A., Komes, D., Karlović, S., Djaković, S., Špoljarić, I., Mršić, G., & Ježek, D. (2015). Improving the controlled delivery formulations of caffeine in alginate hydrogel beads combined with pectin, carrageenan, chitosan and psyllium. *Food Chemistry*, *167*, 378–386.

Bhattarai, S. R., Bahadur K.C., R., Aryal, S., Khil, M. S., & Kim, H. Y. (2007). N-Acylated chitosan stabilized iron oxide nanoparticles as a novel nano-matrix and ceramic modification. *Carbohydrate Polymers*, *69*(3), 467–477.

Burey, P., Bhandari, B. R., Howes, T., & Gidley, M. J. (2008). Hydrocolloid gel particles: formation, characterization, and application. *Critical Reviews in Food Science and Nutrition*, *48*(789190280), 361–377.

Cai, S., Zhao, M., Fang, Y., Nishinari, K., Phillips, G. O., & Jiang, F. (2014). Microencapsulation of Lactobacillus acidophilus CGMCC1.2686 via

ACCEPTED MANUSCRIPT

emulsification/internal gelation of alginate using Ca-EDTA and CaCO3 as calcium sources. *Food Hydrocolloids*, *39*, 295–300.

Chan, E. S., Lee, B. B., Ravindra, P., & Poncelet, D. (2009). Prediction models for shape and size of ca-alginate macrobeads produced through extrusion-dripping method. *Journal of Colloid and Interface Science*, *338*(1), 63–72.

Chew, S. C., & Nyam, K. L. (2016). Microencapsulation of kenaf seed oil by co-extrusion technology. *Journal of Food Engineering*, *175*, 43–50.

Chopra, M., Bernela, M., Kaur, P., Manuja, A., Kumar, B., & Thakur, R. (2015). Alginate/gum acacia bipolymeric nanohydrogels-Promising carrier for Zinc oxide nanoparticles. *International Journal of Biological Macromolecules*, *72*, 827–833.

Costa, P., & Sousa Lobo, J. M. (2001). Modeling and comparison of dissolution profiles. *European Journal of Pharmaceutical Sciences*, *13*(2), 123–133.

Fang, Y., Al-Assaf, S., Phillips, G. O., Nishinari, K., Funami, T., Williams, P. a., & Li, A. (2007). Multiple steps and critical behaviors of the binding of calcium to alginate. *Journal of Physical Chemistry B*, *111*(10), 2456–2462.

Fang, Y., Li, L., Vreeker, R., Yao, X., Wang, J., Ma, Q., Jiang, F., & Phillips, G. O. (2011). Rehydration of dried alginate gel beads: Effect of the presence of gelatin and gum arabic. *Carbohydrate Polymers*, *86*(3), 1145–1150.

Fox, T. G. (1956). Influence of Diluent and of Copolymer Composition on the Glass Temperature of a Polymer System. *Bulletin of the American Physical Society*, *1*, 123.

Gong, R., Li, C., Zhu, S., Zhang, Y., Du, Y., & Jiang, J. (2011). A novel pH-sensitive hydrogel based on dual crosslinked alginate/N-α-glutaric acid chitosan for oral delivery of protein. *Carbohydrate Polymers*, *85*(4), 869–874.

Gouin, S. (2004). Microencapsulation: Industrial appraisal of existing technologies and trends. *Trends in Food Science and Technology*, *15*(7-8), 330–347.

ACCEPTED MANUSCRIPT

Goyeneche, R., Roura, S., Ponce, A., Vega-Gálvez, A., Quispe-Fuentes, I., Uribe, E., & Di Scala, K. (2015). Chemical characterization and antioxidant capacity of red radish (Raphanus sativus L.) leaves and roots. *Journal of Functional Foods*, *16*, 256–264.

Jost, V., Kobsik, K., Schmid, M., & Noller, K. (2014). Influence of plasticiser on the barrier, mechanical and grease resistance properties of alginate cast films. *Carbohydrate Polymers*, *110*, 309–19.

Korsmeyer, R. W., Gurny, R., Doelker, E., Buri, P., & Peppas, N. A. (1983). Mechanisms of solute release from porous hydrophilic polymers. *International Journal of Pharmaceutics*, *15*(1), 25–35.

Koyama, M., & Kitamura, Y. (2014). Development of a new rice beverage by improving the physical stability of rice slurry. *Journal of Food Engineering*, *131*, 89–95.

Lai, L. S., Chou, S. T., & Chao, W. W. (2001). Studies on the antioxidative activities of Hsian-tsao (Mesona procumbens Hemsl) leaf gum. *Journal of Agricultural and Food Chemistry*, *49*(2), 963–968.

Lee, K. Y., & Mooney, D. J. (2012). Alginate: Properties and biomedical applications. *Progress in Polymer Science (Oxford)*, *37*(1), 106–126.

Liu, Z., Ge, X., Lu, Y., Dong, S., Zhao, Y., & Zeng, M. (2012). Effects of chitosan molecular weight and degree of deacetylation on the properties of gelatine-based films. *Food Hydrocolloids*, *26*(1), 311–317.

López Córdoba, A., Deladino, L., & Martino, M. (2013). Effect of starch filler on calcium-alginate hydrogels loaded with yerba mate antioxidants. *Carbohydrate Polymers*, *95*(1), 315–323.

Lozano-Vazquez, G., Lobato-Calleros, C., Escalona-Buendia, H., Chavez, G., Alvarez-Ramirez, J., & Vernon-Carter, E. J. (2015). Effect of the weight ratio of alginate-modified tapioca starch on the physicochemical properties and release kinetics of chlorogenic acid

ACCEPTED MANUSCRIPT

containing beads. *Food Hydrocolloids*, *48*, 301–311.

Lupo, B., Maestro, A., Gutiérrez, J. M., & González, C. (2015). Characterization of alginate beads with encapsulated cocoa extract to prepare functional food: Comparison of two gelation mechanisms. *Food Hydrocolloids*, *49*, 25–34.

Matalanis, A., Jones, O. G., & McClements, D. J. (2011). Structured biopolymer-based delivery systems for encapsulation, protection, and release of lipophilic compounds. *Food Hydrocolloids*, *25*(8), 1865–1880.

Mohy Eldin, M. S., Kamoun, E. a., Sofan, M. a., & Elbayomi, S. M. (2014). l-Arginine grafted alginate hydrogel beads: A novel pH-sensitive system for specific protein delivery. *Arabian Journal of Chemistry*, *8*(3), 355–365.

Mukhopadhyay, P., Chakraborty, S., Bhattacharya, S., Mishra, R., & Kundu, P. P. (2015). pH-sensitive chitosan/alginate core-shell nanoparticles for efficient and safe oral insulin delivery. *International Journal of Biological Macromolecules*, *72*, 640–648.

Nakata, T., Kyoui, D., Takahashi, H., Kimura, B., & Kuda, T. (2016). Inhibitory effects of laminaran and alginate on production of putrefactive compounds from soy protein by intestinal microbiota in vitro and in rats. *Carbohydrate Polymers*, *143*, 61–69.

Nami, Y., Haghshenas, B., & Yari Khosroushahi, A. (2016). Effect of psyllium and gum Arabic biopolymers on the survival rate and storage stability in yogurt of *Enterococcus durans* IW3 encapsulated in alginate. *Food Science & Nutrition*, (August), 1–10.

Nayak, A. K., Das, B., & Maji, R. (2012). Calcium alginate/gum arabic beads containing glibenclamide: Development and in vitro characterization. *International Journal of Biological Macromolecules*, *51*(5), 1070–1078.

Nayak, A. K., Pal, D., & Santra, K. (2016). Swelling and drug release behavior of metformin HCl-loaded tamarind seed polysaccharide-alginate beads. *International Journal of Biological Macromolecules*, *82*, 1023–1027.

ACCEPTED MANUSCRIPT

Pawar, S. N., & Edgar, K. J. (2012). Alginate derivatization: A review of chemistry, properties and applications. *Biomaterials*, *33*(11), 3279–3305.

Pei, K., Ying, Y., & Chu, C. (2017). Molecular dynamic simulations of a new family of synthetic biodegradable amino acid-based poly(ester amide) biomaterials: Glass transition temperature and adhesion behavior. *Materials Today Chemistry*, *4*, 90–96.

Siepmann, J., & Peppas, N. a. (2001). Modeling of drug release from delivery systems based on hydroxypropyl methylcellulose (HPMC). *Advanced Drug Delivery Reviews*, *48*(2-3), 139–157.

Sinha, P., Ubaidulla, U., Hasnain, M. S., Nayak, A. K., & Rama, B. (2015). Alginate-okra gum blend beads of diclofenac sodium from aqueous template using ZnSO4 as a cross-linker. *International Journal of Biological Macromolecules*, *79*, 555–563.

Tonon, R. V., Brabet, C., & Hubinger, M. D. (2010). Anthocyanin stability and antioxidant activity of spray-dried a??ai (Euterpe oleracea Mart.) juice produced with different carrier agents. *Food Research International*, *43*(3), 907–914.

Tsai, F. H., Chiang, P. Y., Kitamura, Y., Kokawa, M., & Khalid, N. (2016). Preparation and physical property assessments of liquid-core hydrogel beads loaded with burdock leaf extracts. *RSC Advances*, *6*, 91361–91369.

Tsai, F. H., Chuang, P. Y., Kitamura, Y., Kokawa, M., & Islam, M. Z. (2017). Producing liquid-core hydrogel beads by reverse spherification: Effect of secondary gelation on physical properties and release characteristics. *Food Hydrocolloids*, *62*, 140–148.

Tsai, F. H., Kitamura, Y., & Kokawa, M. (2017). Liquid-core alginate hydrogel beads loaded with functional compounds of radish by-products by reverse spherification: Optimization by response surface methodology. *International Journal of Biological Macromolecules*, *96*, 600–610.

Wang, Q., Zhang, J., & Wang, A. (2009). Preparation and characterization of a novel pH-

ACCEPTED MANUSCRIPT

sensitive chitosan-g-poly (acrylic acid)/attapulgite/sodium alginate composite hydrogel bead for controlled release of diclofenac sodium. *Carbohydrate Polymers*, *78*(4), 731–737.

Wortmann, F. J., Rigby, D. G., & Phillips, D. G. (1984). Glass Transition Temperature of Wool as a Function of Regain. *Glass Transition Temperature of Wool as a Function of Regain*, *54*(1), 6–8.

Zeeb, B., Saberi, A. H., Weiss, J., & McClements, D. J. (2015). Formation and characterization of filled hydrogel beads based on calcium alginate: Factors influencing nanoemulsion retention and release. *Food Hydrocolloids*, *50*, 27–36.

Zucker, D., Marcus, D., Barenholz, Y., & Goldblum, A. (2009). Liposome drugs' loading efficiency: A working model based on loading conditions and drug's physicochemical properties. *Journal of Controlled Release*, *139*(1), 73–80.

ACCEPTED MANUSCRIPT

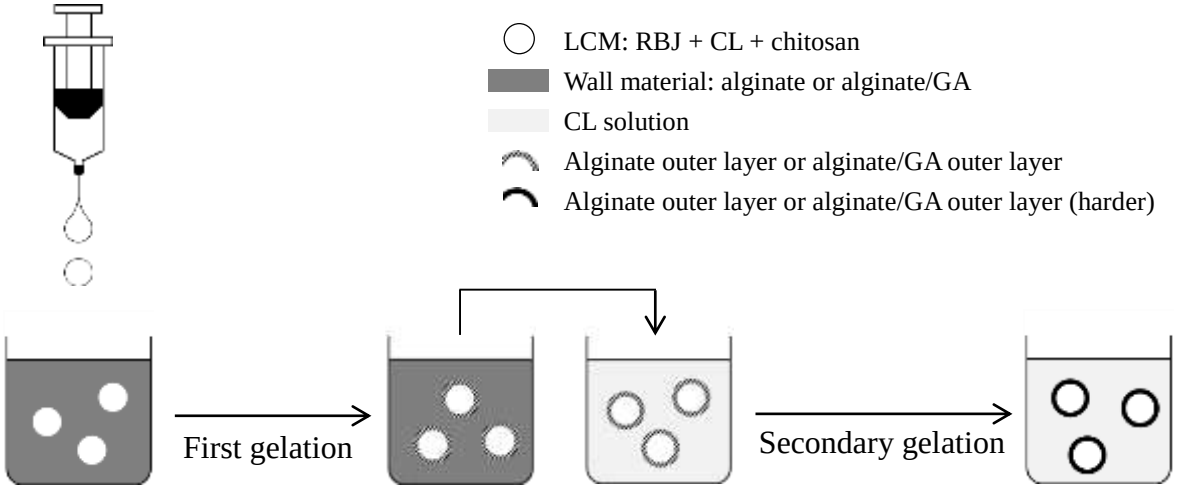

Fig. 1 Formulation of alginate/gum arabic beads by reverse spherification.

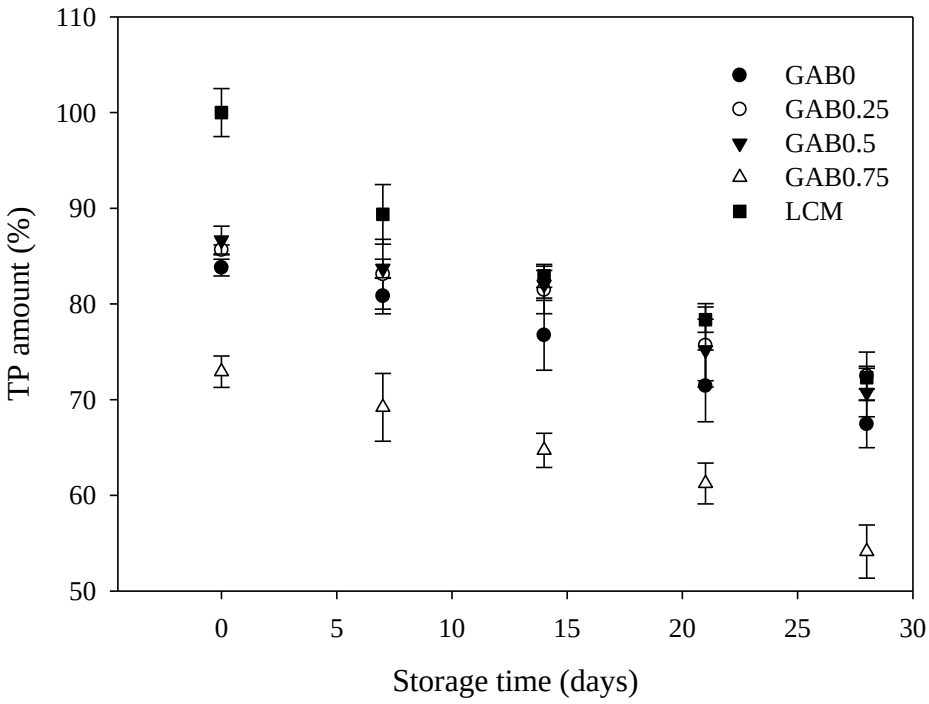

Fig. 2 The amount of total phenolic compounds of alginate/gum arabic beads during storage.

ACCEPTED MANUSCRIPT

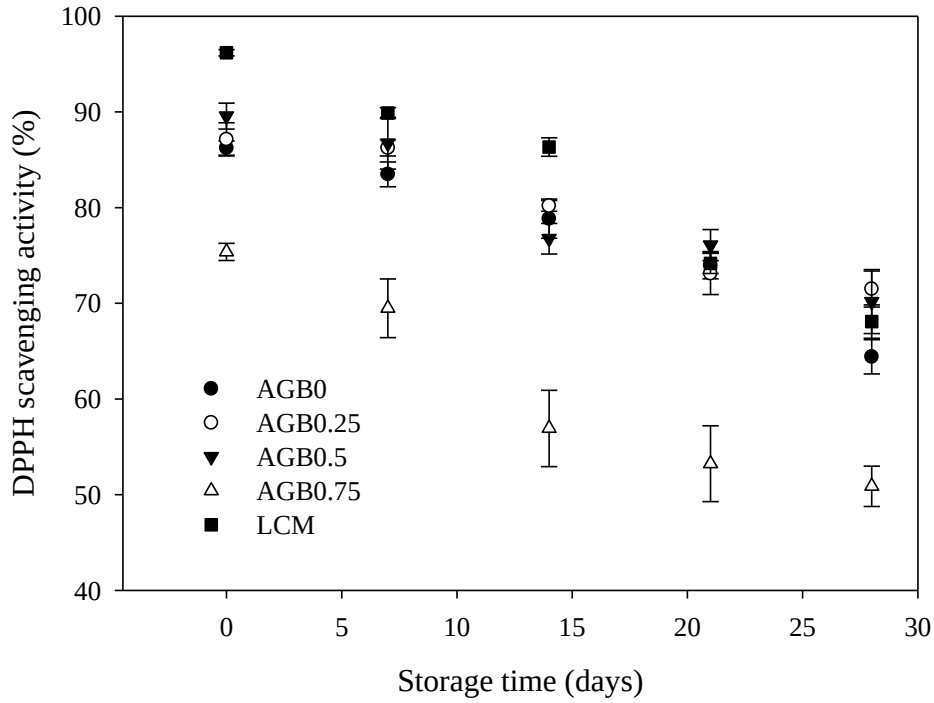

Fig. 3 DPPH scavenging activity of alginate/gum arabic beads during storage.

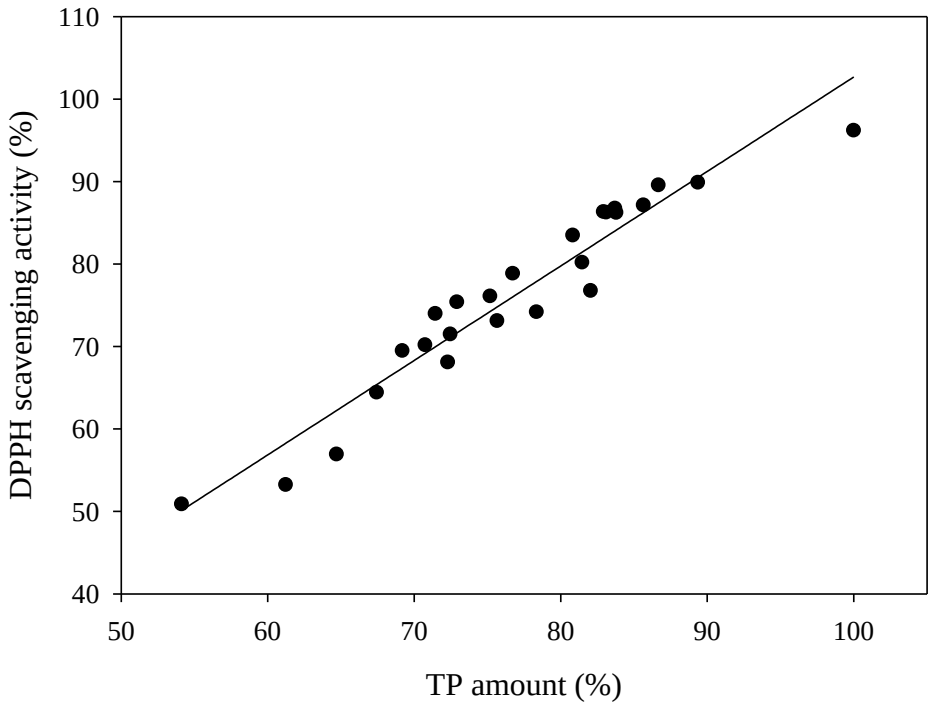

Fig. 4 The correlation between DPPH scavenging activity and the amount of total phenolic compound.

ACCEPTED MANUSCRIPT

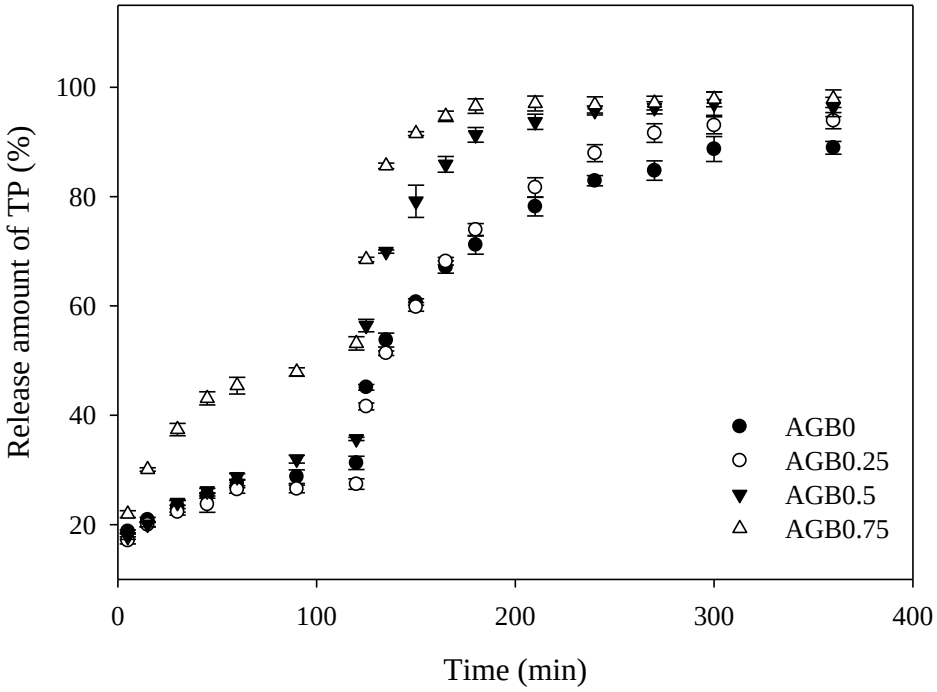

Fig. 5 Total phenolic compounds release from alginate/gum arabic beads in an *in vitro* system.

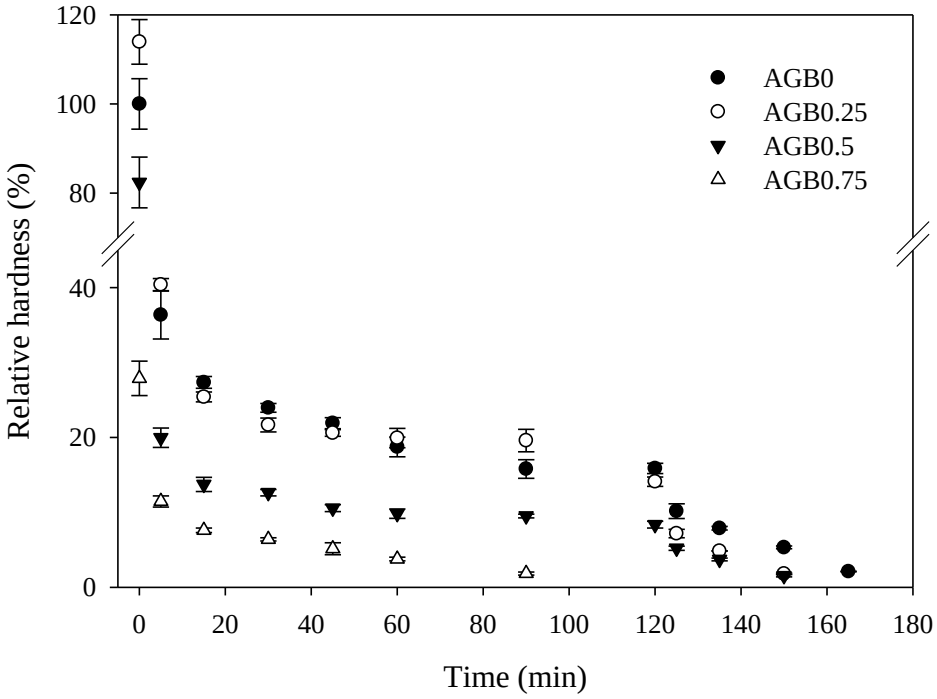

Fig. 6 Hardness of alginate/gum arabic beads in an *in vitro* system.

ACCEPTED MANUSCRIPT

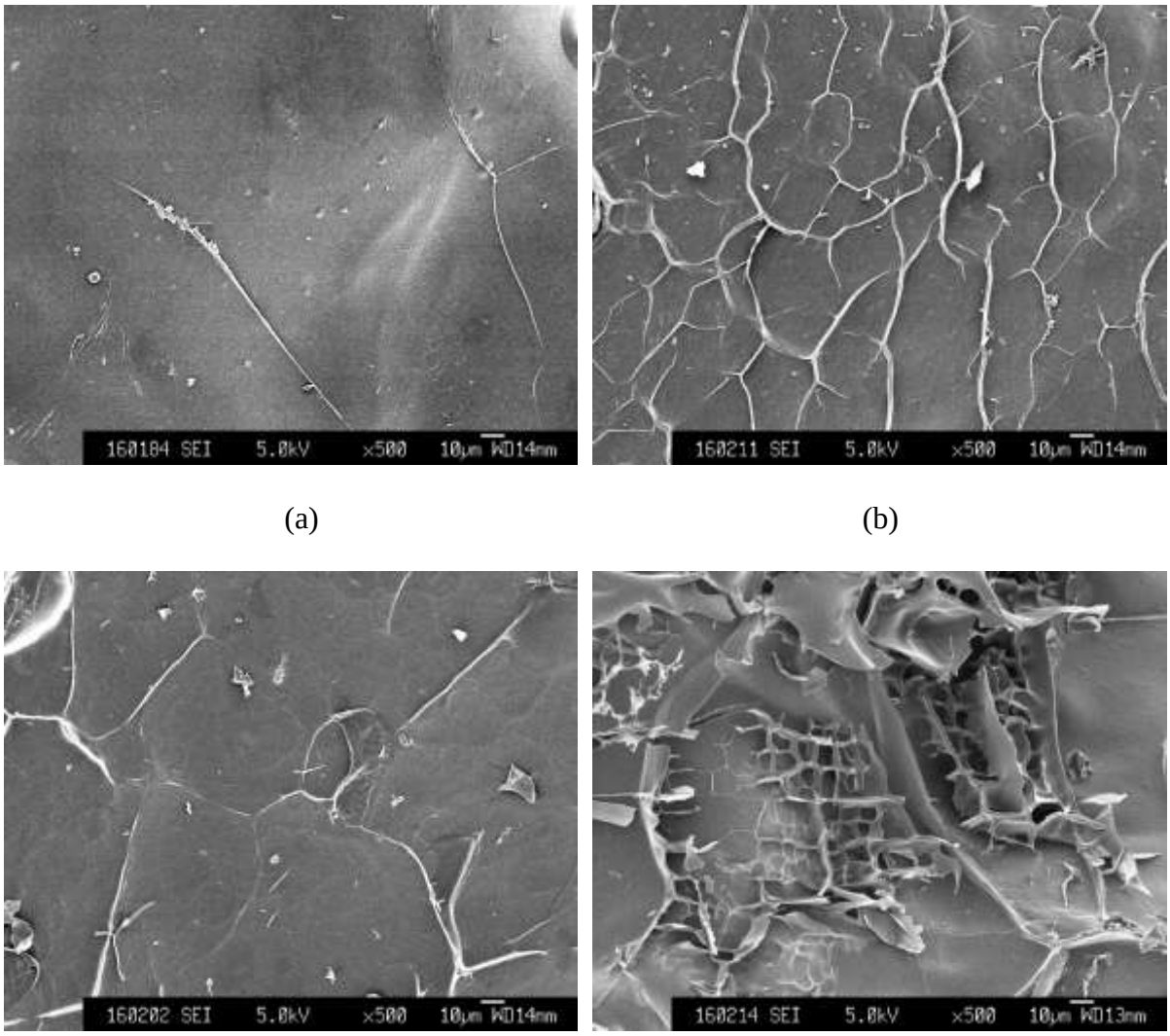

(a) (b)

(c) (d)

Fig. 7 Microstructure of the outer layer of alginate/gum arabic beads. (a) AGB0; (b) AGB 0.25; (c) AGB 0.5; (d) AGB 0.75.

ACCEPTED MANUSCRIPT

Table 1 The formulation of alginate/ gum arabic beads.

Code	Ratio	Gum arabic (g/100mL)	Alginate (g/100mL)
AGB0	0:1	0	1
AGB0.25	0.25:0.75	0.33	1
AGB0.5	0.5:0.5	1	1
AGB0.75	0.75:0.25	3	1

Table 2 Physicochemical properties of alginate/gum arabic beads.

Code	Diameter (mm)	Sphericity ($\times 10^{-2}$)	Loading efficiency (%)	Hardness (N)
AGB0	4.63 ± 0.07^{bc}	3.55 ± 0.22^{a}	83.80 ± 0.87^{b}	23.42 ± 1.32^{b}
AGB0.25	4.58 ± 0.02^{c}	1.36 ± 0.01^{b}	85.65 ± 0.52^{ab}	26.68 ± 1.18^{a}
AGB0.5	4.82 ± 0.09^{b}	1.76 ± 0.29^{b}	86.67 ± 1.45^{a}	19.30 ± 1.34^{c}
AGB0.75	5.66 ± 0.16^{a}	1.34 ± 0.32^{b}	72.91 ± 1.64^{c}	6.53 ± 0.54^{d}

ACCEPTED MANUSCRIPT

Table 3 Kinetic parameters for total phenolic compound degradation and DPPH scavenging ability change during storage.

Code	Total phenolic compound degradation			DPPH scavenging activity		
	k^a (day^{-1})	$t_{1/2}^b$ (day)	R^2	k^a (day^{-1})	$t_{1/2}^b$ (day)	R^2
LCM	1.11×10^{-2}	62.45	0.988	1.26×10^{-2}	55.01	0.961
AGB0	8.00×10^{-3}	86.64	0.987	1.01×10^{-2}	68.63	0.929
AGB0.25	6.10×10^{-3}	113.63	0.957	8.00×10^{-3}	86.64	0.942
AGB0.5	7.30×10^{-3}	94.95	0.969	8.80×10^{-3}	78.77	0.945
AGB0.75	1.03×10^{-2}	67.30	0.986	1.50×10^{-2}	46.20	0.942

[a] *k* represents the kinetic constant of first-order kinetic model.

[b] $t_{1/2}$ represents the half-lives of total phenolic compound degradation or DPPH scavenging activity.

ACCEPTED MANUSCRIPT

Table 4 Kinetic parameters for total phenolic compounds release from alginate/gum arabic beads in an *in vitro* system.

Code	SGF			SIF		
	k^a (min^{-n})	n^a	R^2	k (min^{-n})	n	R^2
AGB0	5.31×10^{-6}	0.162	0.972	2.71×10^{-3}	0.189	0.992
AGB0.25	2.25×10^{-6}	0.155	0.981	4.09×10^{-3}	0.229	0.988
AGB0.5	6.03×10^{-5}	0.221	0.964	5.61×10^{-3}	0.144	0.939
AGB0.75	9.15×10^{-4}	0.278	0.991	6.09×10^{-3}	0.082	0.796

[a] *k* and *n* represents the kinetic constant and release exponent of Korsmeyer-Peppas release kinetics.